

Effects of mean-field momentum dependence on pion production in intermediate-energy heavy-ion collisions

Xin Li^{a,b,*}, Si-Pei Wang^{b,*}, Zhen Zhang^{c,f,*}, Rui Wang^{d,f,*}, Jie Pu^{a,e,f,*}, Chun-Wang Ma^{a,e,f,*}, Lie-Wen Chen^{b,*}

^a*College of Physics, Henan Normal University, Xinxiang, 453007, China*

^b*State Key Laboratory of Dark Matter Physics, Key Laboratory for Particle Astrophysics and Cosmology (MOE), and Shanghai Key Laboratory for Particle Physics and Cosmology, School of Physics and Astronomy, Shanghai Jiao Tong University, Shanghai, 200240, China*

^c*Sino-French Institute of Nuclear Engineering and Technology, Sun Yat-sen University, Zhuhai, 519082, China*

^d*Istituto Nazionale di Fisica Nucleare (INFN), Laboratori Nazionali del Sud, Catania, I-95123, Italy*

^e*Institute of Nuclear Science and Technology, Henan Academy of Sciences, Zhengzhou, 450046, China*

^f*Shanghai Research Center for Theoretical Nuclear Physics, NSFC and Fudan University, Shanghai, 200438, China*

Abstract

Pion production in heavy-ion collisions at intermediate energies provides an important probe of the collision dynamics and nuclear matter equation of state, especially the high-density behavior of the symmetry energy. Using the lattice Boltzmann-Uehling-Uhlenbeck transport model with a recently developed nuclear effective interaction based on the so-called N5LO Skyrme pseudopotential, we investigate the effects of the momentum dependence of nucleon mean-field potentials on the pion production in Au+Au collisions at a beam energy of 1.23 GeV/nucleon. We find that a stronger momentum dependence, for which the nucleon mean-field potentials increase faster with momentum, generally suppresses pion production. This feature can be understood in terms of the mean-field-induced modification of nucleon high-momentum phase space during the compression stage: a stronger momentum dependence can reduce the relative fraction of high-momentum nucleons in heavy-ion collisions, thereby suppressing the production of Δ resonances and pions.

Keywords: Momentum dependence, mean-field potential, Pion production, $NN \leftrightarrow N\Delta$ cross sections

1. Introduction

Heavy-ion collisions (HICs) at intermediate energies (from ~ 100 MeV/nucleon to ~ 1 GeV/nucleon) provide a unique tool to explore the equation of state (EOS) of dense nuclear matter, which lies at the core of both nuclear physics and astrophysics [1–10]. As the lightest hadrons, pions are among the most abundant reaction products in intermediate-energy HICs and carry valuable information on the collision dynamics and nuclear matter EOS. In particular, the charged-pion ratio was proposed as a sensitive probe of the high-density behavior of the nuclear symmetry energy [11], and in the past decades, extensive efforts have been devoted to constraining the density dependence of the symmetry energy from transport model analyses of pion observables [12–21]. However, pronounced model dependence, leading in some cases to controversial conclusions, has been found in various transport model analyses of charged-pion production in Au+Au collisions measured by the FOPI Collaboration [22]. These ambiguities motivate further investigations of pion-production mechanisms in HICs, including Δ potentials [23–25], pion potentials [16, 18, 26–28], threshold

effects [17, 29], energy-conservation effects [25, 30, 31], and short-range correlations [32, 33]. To further quantify uncertainties and improve the predictive power of transport models at these energies, the Transport Model Evaluation Project (TMEP) has also been initiated [34–39].

Recently, the HADES Collaboration has measured charged-pion production in Au+Au collisions at $\sqrt{s_{NN}} = 2.4$ GeV (corresponding to beam energy $E_{beam} = 1.23$ GeV/nucleon) with high-statistics data [40]. These measurements provide an important benchmark for transport model comparisons and can help refine theoretical descriptions of pion production in HICs. Nevertheless, substantial differences between transport-model predictions and the HADES data on pion yields have been observed [40]. Subsequent studies [41, 42] have suggested that in-medium suppression of the Δ -production cross section can help reconcile transport-model calculations with the HADES results. Given the complexity of pion-production mechanisms, further investigation into pion production in HICs at HADES energies remains crucial, especially for constraining nuclear matter EOS with the new data.

Nucleon mean-field potentials are among the most important ingredients in transport models. A key feature of these potentials is their momentum dependence, which arises from the intrinsic momentum dependence of nuclear force, finite-range exchange terms, and other possible contributions [43, 44]. This momentum dependence, which has been clearly demonstrated by nucleon optical-potential measurements, governs essential

*Corresponding author.

Email addresses: lixin20223@stu.hnu.edu.cn (Xin Li), sjtuwsp@gmail.com (Si-Pei Wang), zhangzh275@mail.sysu.edu.cn (Zhen Zhang), rui.wang@lns.infn.it (Rui Wang), wlpupjie@126.com (Jie Pu), machunwang@126.com, machw@htu.edu.cn (Chun-Wang Ma), lwchen@sjtu.edu.cn (Lie-Wen Chen)

phenomena ranging from single-particle motion to collective dynamics in nuclear matter [3, 45–49], and therefore plays a crucial role in the non-equilibrium evolution of nuclear systems. In HICs, a stronger momentum dependence (i.e., nucleon potential rises more steeply with momentum) is expected to lower the fraction of high-momentum nucleons during compression through energy-conservation effects, in a manner analogous to how the symmetry energy regulates the isospin composition of dense matter in *isospin fractionation* [50–52]. This modification of the nucleon momentum distribution, driven by the momentum dependence of nucleon mean field potentials, can significantly influence reaction dynamics and particle production.

In this work we investigate how the momentum dependence of nucleon mean-field potentials influences pion production in Au+Au collisions at HADES energies, by using the lattice Boltzmann-Uehling-Uhlenbeck (LBUU) transport model [53–55] incorporated with the extended Skyrme interactions named N5LO Skyrme pseudopotential [46]. Our results indicate that the momentum dependence of nucleon mean-field potentials can significantly influence pion production.

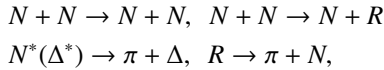
This paper is organized as follow. A brief introduction to the model, particularly the incorporated extended Skyrme interactions with different momentum dependence and the modeling of pion production, is provided in Section 2. We present and discuss our results in Section 3, and conclude with a summary and outlook in Section 4.

2. Methodology

In this work, we employ the LBUU transport model [53–55] to study the nucleon momentum fractionation effects on pion production in Au+Au collisions at $\sqrt{s_{\text{NN}}} = 2.4$ GeV [40]. Within the LBUU model, the time evolution of the one-body phase-space distribution function (Wigner function) $f_\tau = f_\tau(\vec{r}, \vec{p}, t)$ obeys the Boltzmann-Uehling-Uhlenbeck (BUU) equation:

$$(\partial_t + \nabla_p \epsilon_\tau \cdot \nabla_r - \nabla_r \epsilon_\tau \cdot \nabla_p) f_\tau = I_\tau^{\text{coll}} [f_n, f_p, f_\Delta, f_\pi]. \quad (1)$$

Here, τ represents particle species, including neutrons (n), protons (p), the $\Delta(1232)$ resonances, higher-lying resonances N^* and Δ^* up to $N(1720)$ and $\Delta(1950)$, and pions (π). The single-particle energy is denoted by ϵ_τ , and the collision integral I_τ^{coll} includes the following processes and their inverse reactions:



where R denotes resonances including Δ , N^* and Δ^* . In the LBUU model, the mean-field evolution is treated with the lattice Hamiltonian method [54, 56], while the collision integral is handled via the stochastic collision approach [57, 58]. For the initial condition, the Thomas-Fermi initialization [47, 54, 59] provides the nuclear ground state as a static solution of the BUU equation, thereby ensuring evolutionary stability. The present framework of solving the BUU equation has been successfully

Table 1: The macroscopic characteristic quantities of SP10, SP10-FL and SP10-MID. All interactions share the common parameters of $\rho_0 = 0.160 \text{ fm}^{-3}$, $E_0(\rho_0) = -16.0 \text{ MeV}$, $K_0 = 230 \text{ MeV}$, $J_0 = -383 \text{ MeV}$, $I_0 = 1818.9 \text{ MeV}$, $H_0 = -12065 \text{ MeV}$, $E_{\text{sym}}(\rho_0) = 30 \text{ MeV}$, $L = 45 \text{ MeV}$, $K_{\text{sym}} = -110 \text{ MeV}$, $J_{\text{sym}} = 700 \text{ MeV}$, $I_{\text{sym}} = -2458.5 \text{ MeV}$, $H_{\text{sym}} = 19663 \text{ MeV}$.

	SP10	SP10-FL	SP10-MID
$a_0 (\text{MeV})$	-64.97	-64.44	-52.84
$a_2 (\text{MeV fm}^2)$	7.104	6.829	0
$a_4 (\text{MeV fm}^4)$	-0.1628	-0.1719	0
$a_6 (\text{MeV fm}^6)$	1.731×10^{-3}	1.908×10^{-3}	0
$a_8 (\text{MeV fm}^8)$	-8.614×10^{-6}	-9.672×10^{-6}	0
$a_{10} (\text{MeV fm}^{10})$	1.621×10^{-8}	1.827×10^{-8}	0
$b_0 (\text{MeV})$	34.70	34.70	32.43
$b_2 (\text{MeV fm}^2)$	-3.323	-3.323	0
$b_4 (\text{MeV fm}^4)$	2.733×10^{-2}	2.733×10^{-2}	0
$b_6 (\text{MeV fm}^6)$	-8.992×10^{-5}	-8.992×10^{-5}	0
$b_8 (\text{MeV fm}^8)$	1.5849×10^{-7}	1.5849×10^{-7}	0
$b_{10} (\text{MeV fm}^{10})$	-1.738×10^{-10}	-1.738×10^{-10}	0

applied to investigate nuclear collective motions in heavy nuclei [54, 60–62], light-nuclei yields [63, 64] and proton collective flows [46] in HICs at intermediate energies. A more detailed descriptions of the present framework can be found in Ref. [55].

2.1. Extended Skyrme effective interactions

In this work, the baryon mean-field potentials in the LBUU model are derived from the N5LO Skyrme pseudopotential recently developed and implemented in Ref. [46]. Within the framework of N5LO Skyrme pseudopotential, the single-nucleon potential in symmetric nuclear matter and the (first-order) nuclear symmetry potential at saturation density ρ_0 , i.e., U_0 and U_{sym} , take the polynomial momentum-dependent forms

$$U_0(\rho_0, p) \equiv a_0 + a_2 \left(\frac{p}{\hbar} \right)^2 + a_4 \left(\frac{p}{\hbar} \right)^4 + a_6 \left(\frac{p}{\hbar} \right)^6 + a_8 \left(\frac{p}{\hbar} \right)^8 + a_{10} \left(\frac{p}{\hbar} \right)^{10}, \quad (2)$$

and

$$U_{\text{sym}}(\rho_0, p) \equiv b_0 + b_2 \left(\frac{p}{\hbar} \right)^2 + b_4 \left(\frac{p}{\hbar} \right)^4 + b_6 \left(\frac{p}{\hbar} \right)^6 + b_8 \left(\frac{p}{\hbar} \right)^8 + b_{10} \left(\frac{p}{\hbar} \right)^{10}, \quad (3)$$

where the coefficients a_n and b_n ($n = 0, 2, 4, 6, 8, 10$) are determined by the Skyrme parameters. This flexible parameterization allows one to explore systematically the influence of momentum dependence in the baryon mean field on the dynamics of HICs. In particular, the LBUU calculations based on the N5LO Skyrme pseudopotential [46] with empirical parameter values can reasonably reproduce proton flow data in Au+Au collisions at $\sqrt{s_{\text{NN}}} = 2.4$ GeV measured by HADES collaboration [65, 66], demonstrating the essential role of momentum dependence in the dynamics of HICs at GeV energies.

In the following LBUU simulations, we adopt the N5LO Skyrme pseudopotential SP10D02 reported in Ref. [46]

and denoted it by ‘‘SP10’’ here. In addition, based on the SP10, two new interactions, SP10-FL and SP10-MID, with different momentum dependence of single-nucleon potential are constructed following the strategy in Ref. [46]. The 22 adjustable parameters in the adopted extended Skyrme interaction are determined by 12 characteristic quantities for the EOS of symmetric nuclear matter (SNM) $E_0(\rho)$ and the symmetry energy $E_{\text{sym}}(\rho)$, along with 10 coefficients a_n and b_n ($n = 2, 4, 6, 8, 10$) in Eqs. (2) and (3). The 12 EOS characteristic quantities are defined by Taylor expansion coefficients of the $E_0(\rho)$ and $E_{\text{sym}}(\rho)$ at saturation density ρ_0 , including ρ_0 , $E_0(\rho_0)$, $K_0 = 9\rho_0^2[d^2E_0/d\rho^2]|_{\rho=\rho_0}$, $J_0 = 27\rho_0^3[d^3E_0(\rho)/d\rho^3]|_{\rho=\rho_0}$, $I_0 = 81\rho_0^4[d^4E_0(\rho)/d\rho^4]|_{\rho=\rho_0}$, $H_0 = 243\rho_0^5[d^5E_0(\rho)/d\rho^5]|_{\rho=\rho_0}$, $E_{\text{sym}}(\rho_0)$, $L = 3\rho_0[dE_{\text{sym}}(\rho)/d\rho]|_{\rho=\rho_0}$, $K_{\text{sym}} = 9\rho_0^2[d^2E_{\text{sym}}(\rho)/d\rho^2]|_{\rho=\rho_0}$, $J_{\text{sym}} = 27\rho_0^3[d^3E_{\text{sym}}(\rho)/d\rho^3]|_{\rho=\rho_0}$, $I_{\text{sym}} = 81\rho_0^4[d^4E_{\text{sym}}(\rho)/d\rho^4]|_{\rho=\rho_0}$, and $H_{\text{sym}} = 243\rho_0^5[d^5E_{\text{sym}}(\rho)/d\rho^5]|_{\rho=\rho_0}$. For all the three interactions, we set $\rho_0 = 0.160 \text{ fm}^{-3}$, $E_0(\rho_0) = -16.0 \text{ MeV}$, $K_0 = 230 \text{ MeV}$, $J_0 = -383 \text{ MeV}$, $I_0 = 1818.9 \text{ MeV}$, $H_0 = -12065 \text{ MeV}$, $E_{\text{sym}}(\rho_0) = 30 \text{ MeV}$, $L = 45 \text{ MeV}$, $K_{\text{sym}} = -110 \text{ MeV}$, $J_{\text{sym}} = 700 \text{ MeV}$, $I_{\text{sym}} = -2458.5 \text{ MeV}$, $H_{\text{sym}} = 19663 \text{ MeV}$, following SP10D02 [46]. As for the coefficients a_n , they are tuned to fit the empirical optical potential from Hama *et al.* and its extrapolation up to kinetic energy of about 1.5 GeV [67, 68] for SP10, while to reproduce the empirical optical potential by Feldmeier and Lindner (FL) [69] for SP10-FL. Note the coefficients b_n for both SP10 and SP10-FL are set to be the same as those for SP10D02 [46].

For SP10-MID, we set a_2-a_{10} and b_2-b_{10} to be zero, and determine a_0 and b_0 according to the HVH theorem [70–72], which results in momentum-independent single-nucleon potential in nuclear medium. Detailed values for a_n and b_n in the three extended Skyrme interactions are listed in Tab. 1.

Figure 1 (a) compares the energy dependence of single-nucleon potential in SNM at ρ_0 predicted by the three interactions with nucleon optical potential extracted from proton-nucleus scattering data [67]. It is seen that the SP10 and SP10-FL well reproduce the optical potential by Hama *et al.* [67, 68] as well as Feldmeier and Linder [69], respectively. The empirical optical potential from Hama *et al.* and its extrapolation up to kinetic energy of about 1.5 GeV [67, 68] corresponds to the Schrödinger-equivalent potential based on the Dirac phenomenology. The optical potential from Feldmeier and Lindner (FL) in Ref. [69] employs a different definition of the non-relativistic optical potential based on the same Dirac phenomenology of proton scattering data by Hama *et al.* [67]. The different definitions for non-relativistic optical potential lead to distinct energy dependence. We can see that the Hama potential predicts larger optical potentials at high energies, which results in stronger momentum dependence in SP10 than that in SP10-FL. For SP10-MID, the single nucleon potential is momentum/energy independent. As a result, it takes a constant value of $U_0 = -52.84 \text{ MeV}$ in SNM at ρ_0 .

Figure 1 (b) shows proton and neutron potentials in asymmetric nuclear matter at density $\rho = \rho_0$ and isospin asymmetry of $\delta = 0.198$, comparable to that of a ^{197}Au nucleus. As ex-

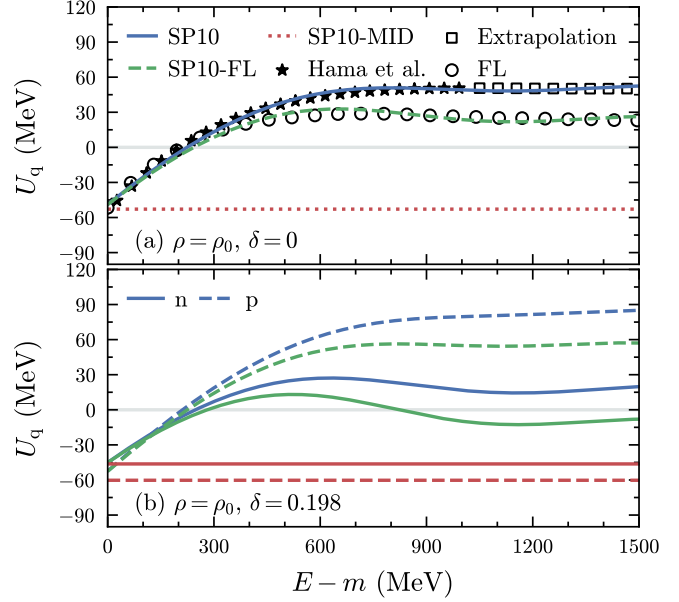


Figure 1: Energy dependence of single-nucleon potential U_q in cold nuclear matter predicted by SP10, SP10-FL and SP10-MID. (a) Results for symmetric nuclear matter ($\delta = 0$) at saturation density ρ_0 are compared with the nucleon optical potential in by Hama *et al.* [67] (solid stars) and its extrapolation to 1.5 GeV (open squares), as well as with the result from Feldmeier and Linder (FL) [69] (open circles). (b) Neutron and proton potentials in asymmetric nuclear matter at density $\rho = \rho_0$ and isospin asymmetry $\delta = 0.198$, a value typical for a ^{197}Au nucleus.

pected, the SP10-MID interaction, being momentum independent, yields constant neutron and proton potentials. In contrast, both SP10 and SP10-FL predict a noticeably stronger momentum dependence for protons than for neutrons, reflecting the positive neutron-proton effective-mass splitting in neutron-rich matter.

For the mean-field potentials of Δ resonances, we note that the isospin dependence of the Δ single-particle potential remains an open question [23, 30, 73, 74]. There are two popular forms: one proposed in Ref. [52] and the other in Ref. [75], and both are expressed as a linear scaling of neutrons (n) and protons (p) potentials. In this work, following Ref. [46], we adopt the relations between Δ and nucleon potentials proposed in Ref. [75], namely, $U_{\Delta^{++}} = -U_n + 2U_p$, $U_{\Delta^+} = U_p$, $U_{\Delta^0} = U_n$, $U_{\Delta^-} = 2U_n - U_p$. As for higher resonances and pions, they are treated as freely propagating particles without mean-field potentials.

2.2. Modeling of pion production

In the present LBUU model, pions are produced through the decays of Δ , N^* and Δ^* resonances. Since Δ decay dominates the final π yield in HICs at intermediate energies, an accurate description of the $N + N \rightarrow N + \Delta$ cross section is critical for transport-model studies of pion production. In this work, we introduce a new parameterization for $p + p \rightarrow n + \Delta^{++}$ cross sections by fitting experimental data from Refs. [76] (CERN8401)

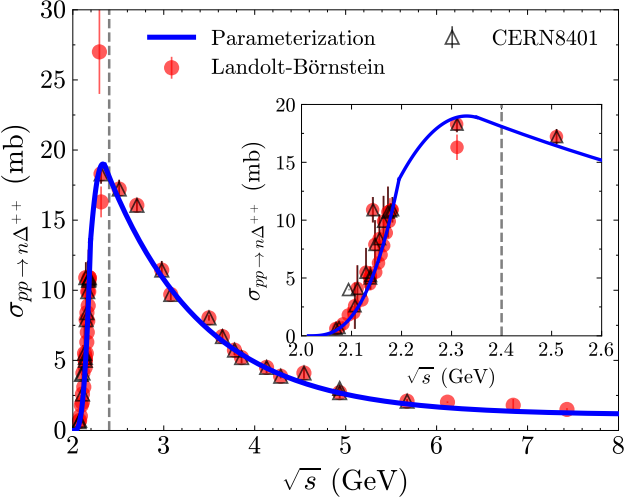


Figure 2: Cross section for $pp \rightarrow n\Delta^{++}$ as a function of the invariant mass \sqrt{s} (in GeV). Experimental data are taken from CERN8401 [76] (black hollow triangles) and Landolt-Börnstein [77] (Red solid dot). The solid blue line represents the parameterization given by Eq. (4). The inset provides an enlarged view of the cross section near threshold, and the black dashed line indicates $\sqrt{s} = 2.4$ GeV.

and [77] (Landolt-Börnstein), i.e.,

$$\sigma_{pp \rightarrow n\Delta^{++}}(\sqrt{s}) = \begin{cases} 1650 \cdot (\sqrt{s} - 2.014)^{2.81}, & \text{for } 2.014 \text{ GeV} < \sqrt{s} \leq 2.20 \text{ GeV} \\ 19 - 300 \cdot (\sqrt{s} - 2.33)^2, & \text{for } 2.20 \text{ GeV} \leq \sqrt{s} \leq 2.35 \text{ GeV} \\ 1.104 + 17.682 \cdot \exp\left(-\frac{\sqrt{s} - 2.357}{0.08}\right), & \text{for } \sqrt{s} \geq 2.35 \text{ GeV} \end{cases} \quad (4)$$

where the invariant mass \sqrt{s} and the cross section $\sigma_{pp \rightarrow n\Delta^{++}}$ are in units of GeV and mb, respectively. As shown in Fig. 2, this parametrization well reproduces the experimental data from threshold up to high energies of ~ 7 GeV. Cross sections for other Δ production channels are related by isospin symmetry as $\sigma_{nn \rightarrow p+\Delta^-}(\sqrt{s}) = \sigma_{pp \rightarrow n\Delta^{++}}(\sqrt{s})$, $\sigma_{pp \rightarrow p+\Delta^0} = \sigma_{nn \rightarrow n+\Delta^0} = \frac{1}{3}\sigma_{pp \rightarrow n\Delta^{++}}(\sqrt{s})$, and $\sigma_{np \rightarrow n+\Delta^+} = \sigma_{np \rightarrow p+\Delta^0} = \frac{2}{3}\sigma_{pp \rightarrow n\Delta^{++}}(\sqrt{s})$. The Δ absorption ($\sigma_{N\Delta \rightarrow NN}$) cross sections are obtained from the corresponding production cross sections by detailed balance condition [57]. For the Δ resonance, we adopt the spectral function, decay width, and absorption cross section from Ref. [39]. The corresponding properties for the Δ^* and N^* resonances are taken from Ref. [78].

It should be noted that, in principle, momentum-dependent mean-field potentials affect not only the reaction dynamics but also the kinematics and the in-medium cross sections and decay widths entering all inelastic scattering and decay channels. In the present work, however, we focus solely on the dynamical impact of the momentum dependence of the nucleon potentials and neglect mean-field potentials in treating collisions. The impact of this momentum dependence on the collision terms, such as threshold effects [17, 29] or in-medium corrections to the NN inelastic cross sections [41, 42], is left for future studies.

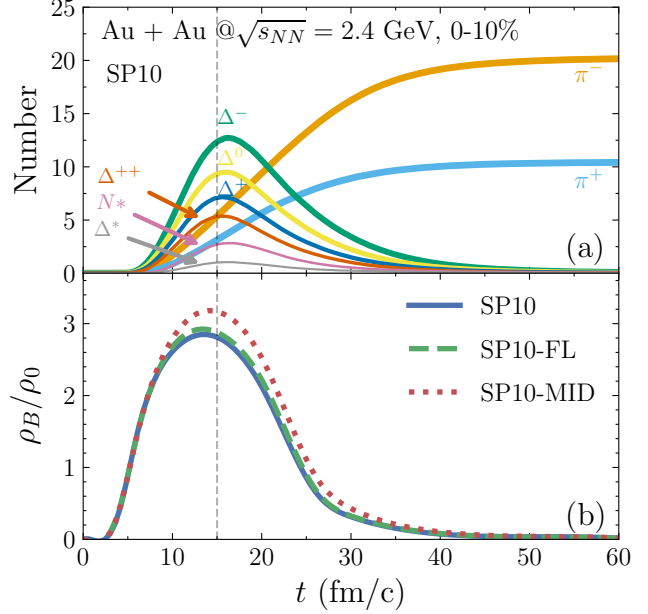


Figure 3: Time evolution of (a) the number of pions (π^- , π^+) and resonances (Δ^- , Δ^0 , Δ^+ , Δ^{++} , N^* , Δ^*) obtained from LBUU calculation using the SP10 interaction, and (b) the central baryon density ρ_B predicted by the SP10, SP10-FL and SP10-MID. Both panels correspond to the Au+Au collisions at $\sqrt{s_{NN}} = 2.4$ GeV and 0-10% centrality. The vertical black dashed lines indicate $t = 15$ fm/c.

To evaluate the momentum dependence effects on pion production, we solve the BUU equation with the three interactions, i.e., SP10, SP10-FL and SP10-MID to simulate the Au+Au collisions at $\sqrt{s_{NN}} = 2.4$ GeV. Some details of the simulations are as follows: the lattice spacing is set to be 1 fm; the gradient parameter $E^{[2]}$ in the Thomas-Fermi initialization for the ground state of ^{197}Au as described in Refs. [46, 54] is set to -310 MeV fm 5 for the interactions SP10, SP10-FL and SP10-MID, to fit the experimental binding energy of ^{197}Au ; the number of test particles is 50,000; the simulation of the reaction is stopped at 60 fm/c, with a time step of 0.2 fm/c; the free nucleon-nucleon elastic cross section $\sigma_{NN}^{\text{free}}$ is based on the parametrization of experimental nucleon-nucleon scattering data [79], and an in-medium correction to σ_{NN}^* is parameterized according to the nuclear giant dipole resonance width [60].

3. Results and discussion

Figure 3 (a) shows the time evolution of the number of charged pions, Δ -resonances, and higher-lying resonances in Au+Au collisions at $\sqrt{s_{NN}} = 2.4$ GeV and centrality 0 – 10% (impact parameter $b = 0$ – 4.7 fm) calculated using the SP10 interaction. As expected, the Δ resonances are produced in much more abundant than the higher-lying N^* and Δ^* , and therefore dominate the production of charged pions. Fig. 3 (b) displays the time evolution of the baryon density ρ_B in a central cell with $1 \times 1 \times 1$ fm 3 obtained from the LBUU simulations using SP10, SP10-FL and SP10-MID. By comparing panels (a) and (b) of Fig. 3, one clearly sees that these resonances and pions are produced during the compressing stage. Both the cen-

Table 2: Predicted charged pion multiplicities for the 0-10% and 20-30% centrality bins from the LBUU model using the SP10, SP10-FL and SP10-MID interactions. Experimental data measured by HADES collaboration are from Ref. [40].

	0-10%		20-30%	
	π^-	π^+	π^-	π^+
HADES	17.2(11)	9.3(7)	8.7(6)	4.7(3)
SP10	20.3	10.5	9.6	4.7
SP10-FL	21.3	11.1	10.2	5.0
SP10-MID	25.6	14.3	12.5	6.7

tral baryon density and resonance numbers reach their maxima around $t = 15$ fm/c. For the three interactions, SP10, SP10-FL and SP10-MID, the maximum baryon densities are about $2.9\rho_0$, $2.95\rho_0$ and $3.2\rho_0$, respectively. We can see that stronger momentum dependence, as in SP10, not only reduces the maximum achievable density but also causes it to decrease more rapidly over time. This suggests that a stronger momentum dependence is associated with a more anisotropic compression with a larger squeeze-out pressure (and thus a larger magnitude of nucleon elliptic flows), which enhances particle emission and shortens the compression stage.

In Figs. 4 (a) and (b), we further show the rapidity distributions of charged pions in the 0-10% and 20 – 30% centrality bins predicted by the LBUU simulations with the SP10, SP10-FL and SP10-MID interactions. For reference, HADES data [40] are plotted as open circles, and the corresponding integrated yields are listed in Tab. 2. A comparison of results from the three interactions shows the pion yield is strongly sensitive to the momentum-dependence of the nucleon mean-field potential. In particular, in central (centrality 0–10%) collisions, the momentum-independent SP10-MID interaction significantly enhances pion production, giving yields about 29.6% and 23.1% larger than those of SP10 and SP10-FL, respectively. While the difference between SP10 and SP10-FL remains modest, about 5.8%. These results indicate that stronger momentum dependence systematically suppresses pion production. The overall consistency of the SP10 predictions with the HADES measurements seems to further supports the need for a stronger momentum-dependent nucleon potential.

The sensitivity of pion yields to the momentum dependence of the nucleon mean-field potential can be understood from the impact of the momentum dependence on nucleon dynamics. As shown in Fig. 3, a stronger momentum dependence lowers both the maximum density of the compressed nuclear matter formed in the collision and the duration of the compression stage, thereby reducing the number of binary collisions and consequently pion production. More importantly, the momentum-dependent potential decreases the kinetic energy of a nucleon as the nucleon moves into dense nuclear medium, leading to a smaller fraction of high-momentum nucleons during compression. To illustrate this mechanism, we analyze the single time step centered at $t = 15$ fm/c and calculate the average invariant mass $\langle \sqrt{s} \rangle$ for $N + N \rightarrow N + \Delta$ reaction as a function of local baryon density ρ_B in the LBUU simulations

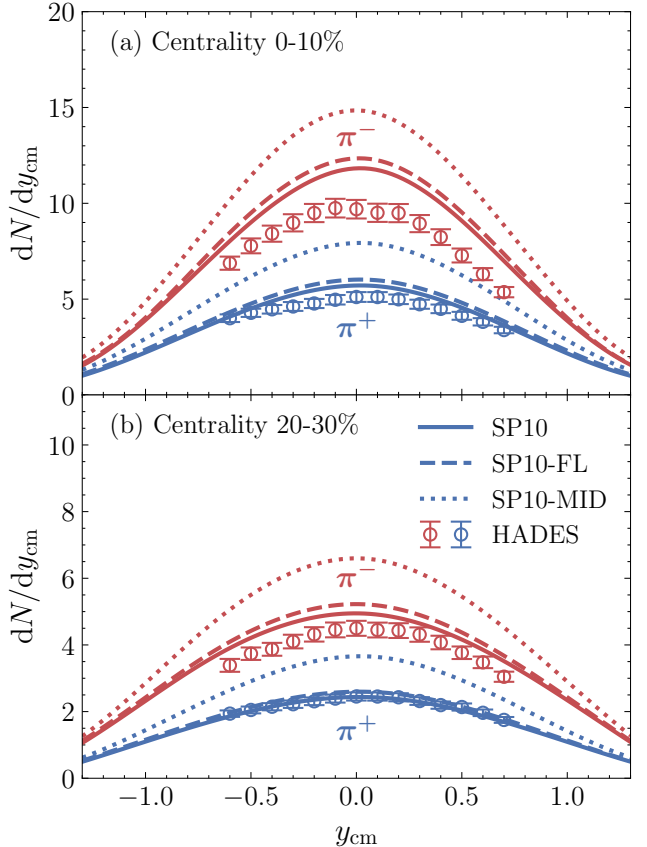


Figure 4: Rapidity distributions of pions with different momentum dependence interactions: SP10, SP10-FL, and SP10-MID in Au + Au collisions at $\sqrt{s_{\text{NN}}} = 2.4$ GeV. Panel (a) shows the results for centrality 0 – 10% and panel (b) for centrality 20-30%. The solid, dashed and dotted curves represent LBUU model predictions, and the symbols represent the HADES experimental data [40] with error bars indicating uncertainties.

with the three interactions, SP10, SP10-FL and SP10-MID. For each of the colliding nucleon pairs in that time step, we compute $s = (p_{1,\text{free}} + p_{2,\text{free}})^2$ with free momenta $p_{i,\text{free}} = (\sqrt{m^2 + \mathbf{p}_i^2}, \mathbf{p}_i)$, and record the local ρ_B at the collision point. The pairs are then grouped by ρ_B , and $\langle \sqrt{s} \rangle$ is evaluated within each density bin. The results are shown in Fig. 5 for central Au+Au collisions (centrality 0-10%). One can see that stronger momentum dependence results in a lower average invariant mass in nucleon-nucleon (NN) scattering. Since the NN inelastic scattering cross section is highly sensitive to the invariant mass near threshold (see Fig. 2), this effect further suppresses pion production.

As we have mentioned before, the pion production in intermediate-energy HICs involves a variety of complex mechanisms. A fully quantitative description of pion production and a reliable extraction of nucleon dynamics from pion observables require more sophisticated and systematic modeling. In fact, one sees from Fig. 4 that the SP10 still over-predicts the π^- yield, especially for the central collisions of 0-10% centrality. Nevertheless, we would like to emphasize that the present work does not attempt a comprehensive quantitative study; in-

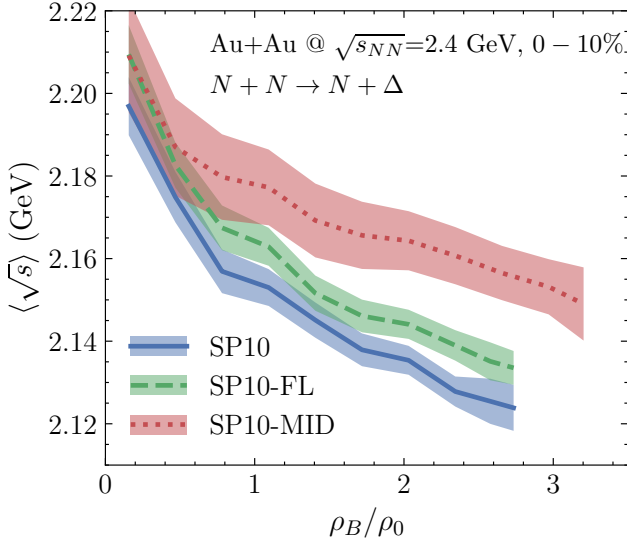


Figure 5: The averaging invariant mass $\langle \sqrt{s} \rangle$ in $N + N \rightarrow N + \Delta$ reaction as functions of baryon density ρ_B at the evolution time of $t = 15$ fm/c obtained from the LBUU simulations with the SP10, SP10-FL, and SP10-MID interactions, respectively. Statistical errors are displayed as the shaded bands.

stead, we focus on a qualitative investigation of the influence of the momentum dependence of nucleon mean-field potentials on the pion yield.

Finally, we note that although the mechanism discussed here differs from that of isospin fractionation in Refs. [50, 52], there is a conceptual analogy. Isospin fractionation is driven by the density dependence of the symmetry energy and leads to a spatial separation of neutrons and protons. In contrast, the effect emphasized in this work originates from the momentum dependence of the nucleon mean-field potential, which modifies the fraction of high-momentum nucleons and thus alters the reaction dynamics in heavy-ion collisions. This change in the fraction of high-momentum nucleons can leave clear signatures in various observables, most notably in the final pion yields. For subthreshold particle production, the effect is expected to be particularly important when the nucleon mean-field potential exhibits a strong momentum dependence.

4. Summary and outlook

We have investigated how the momentum dependence of the nucleon mean-field potential influences pion production in intermediate-energy HICs by using the lattice Boltzmann-Uehling-Uhlenbeck transport model with extended Skyrme interactions named N5LO Skyrme pseudopotential. Three representative interactions, SP10, SP10-FL, and SP10-MID, are constructed to span the range from strong to vanishing momentum dependence. Employing an updated $NN \rightarrow N\Delta$ cross section and simulating Au+Au reactions at $\sqrt{s_{NN}} = 2.4$ GeV, we find that stronger momentum dependence systematically suppresses pion yields, while weaker or momentum-independent mean fields enhance them.

A detailed dynamical analysis reveals that the suppression of the pion yield originates from the modification of nucleon

momentum distributions, namely, a stronger momentum dependence in the nucleon mean-field potentials lowers the fraction of high-momentum nucleons during the compression in heavy-ion collisions, thereby reducing the average invariant mass in nucleon-nucleon inelastic scattering and, consequently, the production of Δ -resonances and pions.

These findings underscore the importance of the momentum-dependence of nucleon potentials in the studies of intermediate-energy HICs. They further highlight mean-field-induced modification of nucleon high-momentum phase space as a key microscopic mechanism that links the momentum dependence of the nuclear mean field to pion observables and, ultimately, to constraints on the high-density nuclear matter equation of state.

Acknowledgements

This work was supported in part by the National Natural Science Foundation of China under Grant Nos. 12235010 and 12147101, the National SKA Program of China (Grant No. 2020SKA0120300), the Science and Technology Commission of Shanghai Municipality (Grant No. 23JC1402700), and the Natural Science Foundation of Henan Province (Grant No. 242300421048).

References

- [1] B.-A. Li, C. M. Ko, W. Bauer, Isospin physics in heavy ion collisions at intermediate-energies, *Int. J. Mod. Phys. E* 7 (1998) 147–230. [arXiv:nucl-th/9707014](https://arxiv.org/abs/nucl-th/9707014), doi: 10.1142/S0218301398000087.
- [2] J. M. Lattimer, M. Prakash, Nuclear matter and its role in supernovae, neutron stars and compact object binary mergers, *Phys. Rept.* 333 (2000) 121–146. [arXiv:astro-ph/0002203](https://arxiv.org/abs/astro-ph/0002203), doi: 10.1016/S0370-1573(00)00019-3.
- [3] P. Danielewicz, R. Lacey, W. G. Lynch, Determination of the equation of state of dense matter, *Science* 298 (2002) 1592–1596. [arXiv:nucl-th/0208016](https://arxiv.org/abs/nucl-th/0208016), doi: 10.1126/science.1078070.
- [4] J. M. Lattimer, M. Prakash, The physics of neutron stars, *Science* 304 (2004) 536–542. [arXiv:astro-ph/0405262](https://arxiv.org/abs/astro-ph/0405262), doi: 10.1126/science.1090720.
- [5] A. W. Steiner, M. Prakash, J. M. Lattimer, P. J. Ellis, Isospin asymmetry in nuclei and neutron stars, *Phys. Rept.* 411 (2005) 325–375. [arXiv:nucl-th/0410066](https://arxiv.org/abs/nucl-th/0410066), doi: 10.1016/j.physrep.2005.02.004.
- [6] V. Baran, M. Colonna, V. Greco, M. Di Toro, Reaction dynamics with exotic beams, *Phys. Rept.* 410 (2005) 335–466. [arXiv:nucl-th/0412060](https://arxiv.org/abs/nucl-th/0412060), doi: 10.1016/j.physrep.2004.12.004.
- [7] B.-A. Li, L.-W. Chen, C. M. Ko, Recent Progress and New Challenges in Isospin Physics with Heavy-Ion Reactions, *Phys. Rept.* 464 (2008) 113–281. [arXiv:0804.3580](https://arxiv.org/abs/0804.3580), doi: 10.1016/j.physrep.2008.04.005.

- [8] M. Oertel, M. Hempel, T. Klähn, S. Typel, Equations of state for supernovae and compact stars, *Rev. Mod. Phys.* 89 (1) (2017) 015007. [arXiv:1610.03361](https://arxiv.org/abs/1610.03361), doi:10.1103/RevModPhys.89.015007.
- [9] A. Sorensen, et al., Dense nuclear matter equation of state from heavy-ion collisions, *Prog. Part. Nucl. Phys.* 134 (2024) 104080. [arXiv:2301.13253](https://arxiv.org/abs/2301.13253), doi:10.1016/j.ppnp.2023.104080.
- [10] J. Chen, et al., Properties of the QCD matter: review of selected results from the relativistic heavy ion collider beam energy scan (RHIC BES) program, *Nucl. Sci. Tech.* 35 (12) (2024) 214. [arXiv:2407.02935](https://arxiv.org/abs/2407.02935), doi:10.1007/s41365-024-01591-2.
- [11] B.-A. Li, Probing the high density behavior of nuclear symmetry energy with high-energy heavy ion collisions, *Phys. Rev. Lett.* 88 (2002) 192701. [arXiv:nucl-th/0205002](https://arxiv.org/abs/nucl-th/0205002), doi:10.1103/PhysRevLett.88.192701.
- [12] Z. Xiao, B.-A. Li, L.-W. Chen, G.-C. Yong, M. Zhang, Circumstantial Evidence for a Soft Nuclear Symmetry Energy at Suprasaturation Densities, *Phys. Rev. Lett.* 102 (2009) 062502. [arXiv:0808.0186](https://arxiv.org/abs/0808.0186), doi:10.1103/PhysRevLett.102.062502.
- [13] Z.-Q. Feng, G.-M. Jin, Probing high-density behavior of symmetry energy from pion emission in heavy-ion collisions, *Phys. Lett. B* 683 (2010) 140–144. [arXiv:0904.2990](https://arxiv.org/abs/0904.2990), doi:10.1016/j.physletb.2009.12.006.
- [14] W.-J. Xie, J. Su, L. Zhu, F.-S. Zhang, Symmetry energy and pion production in the Boltzmann-Langevin approach, *Phys. Lett. B* 718 (2013) 1510–1514. doi:10.1016/j.physletb.2012.12.021.
- [15] J. Xu, L.-W. Chen, C. M. Ko, B.-A. Li, Y.-G. Ma, Energy dependence of pion in-medium effects on the π^-/π^+ ratio in heavy-ion collisions, *Phys. Rev. C* 87 (6) (2013) 067601. [arXiv:1305.0091](https://arxiv.org/abs/1305.0091), doi:10.1103/PhysRevC.87.067601.
- [16] J. Hong, P. Danielewicz, Subthreshold pion production within a transport description of central Au + Au collisions, *Phys. Rev. C* 90 (2) (2014) 024605. [arXiv:1307.7654](https://arxiv.org/abs/1307.7654), doi:10.1103/PhysRevC.90.024605.
- [17] T. Song, C. M. Ko, Modifications of the pion-production threshold in the nuclear medium in heavy ion collisions and the nuclear symmetry energy, *Phys. Rev. C* 91 (1) (2015) 014901. doi:10.1103/PhysRevC.91.014901.
- [18] Z. Zhang, C. M. Ko, Medium effects on pion production in heavy ion collisions, *Phys. Rev. C* 95 (6) (2017) 064604. [arXiv:1701.06682](https://arxiv.org/abs/1701.06682), doi:10.1103/PhysRevC.95.064604.
- [19] Z. Zhang, C. M. Ko, Pion production in a transport model based on mean fields from chiral effective field theory, *Phys. Rev. C* 98 (5) (2018) 054614. doi:10.1103/PhysRevC.98.054614.
- [20] N. Ikeno, A. Ono, Y. Nara, A. Ohnishi, Probing neutron-proton dynamics by pions, *Phys. Rev. C* 93 (4) (2016) 044612, [Erratum: *Phys. Rev. C* 97, 069902 (2018)]. [arXiv:1601.07636](https://arxiv.org/abs/1601.07636), doi:10.1103/PhysRevC.93.044612.
- [21] J. Estee, et al., Probing the Symmetry Energy with the Spectral Pion Ratio, *Phys. Rev. Lett.* 126 (16) (2021) 162701. [arXiv:2103.06861](https://arxiv.org/abs/2103.06861), doi:10.1103/PhysRevLett.126.162701.
- [22] W. Reisdorf, et al., Systematics of pion emission in heavy ion collisions in the 1A- GeV regime, *Nucl. Phys. A* 781 (2007) 459–508. [arXiv:nucl-ex/0610025](https://arxiv.org/abs/nucl-ex/0610025), doi:10.1016/j.nuclphysa.2006.10.085.
- [23] B.-A. Li, Symmetry potential of $\Delta(1232)$ resonance and its effects on the π^-/π^+ ratio in heavy-ion collisions near the pion-production threshold, *Phys. Rev. C* 92 (3) (2015) 034603. [arXiv:1507.03279](https://arxiv.org/abs/1507.03279), doi:10.1103/PhysRevC.92.034603.
- [24] M. D. Cozma, M. B. Tsang, In-medium $\Delta(1232)$ potential, pion production in heavy-ion collisions and the symmetry energy, *Eur. Phys. J. A* 57 (11) (2021) 309. [arXiv:2101.08679](https://arxiv.org/abs/2101.08679), doi:10.1140/epja/s10050-021-00616-3.
- [25] N. Ikeno, A. Ono, Collision integral with momentum-dependent potentials and its impact on pion production in heavy-ion collisions, *Phys. Rev. C* 108 (4) (2023) 044601. [arXiv:2307.02395](https://arxiv.org/abs/2307.02395), doi:10.1103/PhysRevC.108.044601.
- [26] W.-M. Guo, G.-C. Yong, H. Liu, W. Zuo, Effects of pion potential and nuclear symmetry energy on the π^-/π^+ ratio in heavy-ion collisions at beam energies around the pion production threshold, *Phys. Rev. C* 91 (5) (2015) 054616. [arXiv:1410.4926](https://arxiv.org/abs/1410.4926), doi:10.1103/PhysRevC.91.054616.
- [27] Z.-Q. Feng, W.-J. Xie, P.-H. Chen, J. Chen, G.-M. Jin, In-medium and isospin effects on particle production near threshold energies in heavy-ion collisions, *Phys. Rev. C* 92 (4) (2015) 044604. [arXiv:1509.04792](https://arxiv.org/abs/1509.04792), doi:10.1103/PhysRevC.92.044604.
- [28] M. D. Cozma, Constraining the density dependence of the symmetry energy using the multiplicity and average p_T ratios of charged pions, *Phys. Rev. C* 95 (1) (2017) 014601. [arXiv:1603.00664](https://arxiv.org/abs/1603.00664), doi:10.1103/PhysRevC.95.014601.
- [29] G. Ferini, M. Colonna, T. Gaitanos, M. Di Toro, Aspects of particle production in charge asymmetric matter, *Nucl. Phys. A* 762 (2005) 147–166. [arXiv:nucl-th/0504032](https://arxiv.org/abs/nucl-th/0504032), doi:10.1016/j.nuclphysa.2005.08.007.
- [30] M. D. Cozma, The impact of energy conservation in transport models on the π^-/π^+ multiplicity ratio in heavy-ion collisions and the symmetry energy, *Phys. Lett. B* 753

- (2016) 166–172. [arXiv:1409.3110](https://arxiv.org/abs/1409.3110), doi:10.1016/j.physletb.2015.12.015.
- [31] Z. Zhang, C. M. Ko, Effects of energy conservation on equilibrium properties of hot asymmetric nuclear matter, *Phys. Rev. C* 97 (1) (2018) 014610. [arXiv:1712.03286](https://arxiv.org/abs/1712.03286), doi:10.1103/PhysRevC.97.014610.
- [32] B.-A. Li, W.-J. Guo, Z. Shi, Effects of the kinetic symmetry energy reduced by short-range correlations in heavy-ion collisions at intermediate energies, *Phys. Rev. C* 91 (4) (2015) 044601. [arXiv:1408.6415](https://arxiv.org/abs/1408.6415), doi:10.1103/PhysRevC.91.044601.
- [33] G.-C. Yong, Constraining nucleon high momentum in nuclei, *Phys. Lett. B* 765 (2017) 104–108. [arXiv:1503.08523](https://arxiv.org/abs/1503.08523), doi:10.1016/j.physletb.2016.12.013.
- [34] J. Xu, et al., Understanding transport simulations of heavy-ion collisions at 100A and 400A MeV: Comparison of heavy-ion transport codes under controlled conditions, *Phys. Rev. C* 93 (4) (2016) 044609. [arXiv:1603.08149](https://arxiv.org/abs/1603.08149), doi:10.1103/PhysRevC.93.044609.
- [35] Y.-X. Zhang, et al., Comparison of heavy-ion transport simulations: Collision integral in a box, *Phys. Rev. C* 97 (3) (2018) 034625. [arXiv:1711.05950](https://arxiv.org/abs/1711.05950), doi:10.1103/PhysRevC.97.034625.
- [36] M. Colonna, et al., Comparison of heavy-ion transport simulations: Mean-field dynamics in a box, *Phys. Rev. C* 104 (2) (2021) 024603. [arXiv:2106.12287](https://arxiv.org/abs/2106.12287), doi:10.1103/PhysRevC.104.024603.
- [37] H. Wolter, et al., Transport model comparison studies of intermediate-energy heavy-ion collisions, *Prog. Part. Nucl. Phys.* 125 (2022) 103962. [arXiv:2202.06672](https://arxiv.org/abs/2202.06672), doi:10.1016/j.ppnp.2022.103962.
- [38] A. Ono, et al., Comparison of heavy-ion transport simulations: Collision integral with pions and Δ resonances in a box, *Phys. Rev. C* 100 (4) (2019) 044617. [arXiv:1904.02888](https://arxiv.org/abs/1904.02888), doi:10.1103/PhysRevC.100.044617.
- [39] J. Xu, et al., Comparing pion production in transport simulations of heavy-ion collisions at 270AMeV under controlled conditions, *Phys. Rev. C* 109 (4) (2024) 044609. [arXiv:2308.05347](https://arxiv.org/abs/2308.05347), doi:10.1103/PhysRevC.109.044609.
- [40] J. Adamczewski-Musch, et al., Charged-pion production in **Au + Au** collisions at $\sqrt{s_{NN}} = 2.4$ GeV: HADES Collaboration, *Eur. Phys. J. A* 56 (10) (2020) 259. [arXiv:2005.08774](https://arxiv.org/abs/2005.08774), doi:10.1140/epja/s10050-020-00237-2.
- [41] K. Godbey, Z. Zhang, J. W. Holt, C. M. Ko, Charged pion production from Au + Au collisions at sNN=2.4 GeV in the relativistic Vlasov-Uehling-Uhlenbeck model, *Phys. Lett. B* 829 (2022) 137134. [arXiv:2107.13384](https://arxiv.org/abs/2107.13384), doi:10.1016/j.physletb.2022.137134.
- [42] C. Kummer, K. Gallmeister, L. von Smekal, Medium modification of pion production in low-energy Au+Au collisions, *Phys. Rev. C* 109 (5) (2024) 054901. [arXiv:2309.09042](https://arxiv.org/abs/2309.09042), doi:10.1103/PhysRevC.109.054901.
- [43] J. Decharge, D. Gogny, Hartree-Fock-Bogolyubov calculations with the D1 effective interactions on spherical nuclei, *Phys. Rev. C* 21 (1980) 1568–1593. doi:10.1103/PhysRevC.21.1568.
- [44] R. B. Wiringa, Single-particle potential in dense nuclear matter, *Phys. Rev. C* 38 (1988) 2967–2970. doi:10.1103/PhysRevC.38.2967.
- [45] Y.-Y. Liu, J.-P. Yang, Y.-J. Wang, Q.-F. Li, Z.-X. Li, C.-J. Xia, Y.-X. Zhang, A perspective on describing nucleonic flow and pionic observables within the ultra-relativistic quantum molecular dynamics model, *Nucl. Sci. Tech.* 36 (3) (2025) 45. doi:10.1007/s41365-024-01607-x.
- [46] S.-P. Wang, X. Li, R. Wang, J.-T. Ye, L.-W. Chen, Extended Skyrme effective interactions with higher-order momentum dependence for transport models and neutron stars, *Phys. Rev. C* 111 (5) (2025) 054605. [arXiv:2412.09393](https://arxiv.org/abs/2412.09393), doi:10.1103/PhysRevC.111.054605.
- [47] P. Danielewicz, Determination of the mean field momentum dependence using elliptic flow, *Nucl. Phys. A* 673 (2000) 375–410. [arXiv:nucl-th/9912027](https://arxiv.org/abs/nucl-th/9912027), doi:10.1016/S0375-9474(00)00083-X.
- [48] B.-A. Li, B.-J. Cai, L.-W. Chen, J. Xu, Nucleon Effective Masses in Neutron-Rich Matter, *Prog. Part. Nucl. Phys.* 99 (2018) 29–119. [arXiv:1801.01213](https://arxiv.org/abs/1801.01213), doi:10.1016/j.ppnp.2018.01.001.
- [49] J. Rizzo, M. Colonna, M. Di Toro, V. Greco, Transport properties of isospin effective mass splitting, *Nucl. Phys. A* 732 (2004) 202–217. [arXiv:nucl-th/0309032](https://arxiv.org/abs/nucl-th/0309032), doi:10.1016/j.nuclphysa.2003.11.057.
- [50] B.-A. Li, Neutron proton differential flow as a probe of isospin dependence of nuclear equation of state, *Phys. Rev. Lett.* 85 (2000) 4221–4224. [arXiv:nucl-th/0009069](https://arxiv.org/abs/nucl-th/0009069), doi:10.1103/PhysRevLett.85.4221.
- [51] H. S. Xu, et al., Isospin fractionation in nuclear multifragmentation, *Phys. Rev. Lett.* 85 (2000) 716–719. [arXiv:nucl-ex/9910019](https://arxiv.org/abs/nucl-ex/9910019), doi:10.1103/PhysRevLett.85.716.
- [52] B.-A. Li, High density behavior of nuclear symmetry energy and high-energy heavy ion collisions, *Nucl. Phys. A* 708 (2002) 365–390. [arXiv:nucl-th/0206053](https://arxiv.org/abs/nucl-th/0206053), doi:10.1016/S0375-9474(02)01018-7.
- [53] R. Wang, L.-W. Chen, Y. Zhou, Extended Skyrme interactions for transport model simulations of heavy-ion collisions, *Phys. Rev. C* 98 (5) (2018) 054618. [arXiv:1806.03278](https://arxiv.org/abs/1806.03278), doi:10.1103/PhysRevC.98.054618.

- [54] R. Wang, L.-W. Chen, Z. Zhang, Nuclear collective dynamics in the lattice Hamiltonian Vlasov method, *Phys. Rev. C* 99 (4) (2019) 044609. [arXiv:1902.01256](https://arxiv.org/abs/1902.01256), doi: 10.1103/PhysRevC.99.044609.
- [55] R. Wang, Z. Zhang, L.-W. Chen, Y.-G. Ma, Nuclear Collective Dynamics in Transport Model With the Lattice Hamiltonian Method, *Front. in Phys.* 8 (2020) 330. [arXiv:2010.07790](https://arxiv.org/abs/2010.07790), doi:10.3389/fphy.2020.00330.
- [56] R. J. Lenk, V. R. Pandharipande, Nuclear mean field dynamics in the lattice Hamiltonian Vlasov method, *Phys. Rev. C* 39 (1989) 2242–2249. doi:10.1103/PhysRevC.39.2242.
- [57] P. Danielewicz, G. F. Bertsch, Production of deuterons and pions in a transport model of energetic heavy ion reactions, *Nucl. Phys. A* 533 (1991) 712–748. doi: 10.1016/0375-9474(91)90541-D.
- [58] Z. Xu, C. Greiner, Thermalization of gluons in ultrarelativistic heavy ion collisions by including three-body interactions in a parton cascade, *Phys. Rev. C* 71 (2005) 064901. [arXiv:hep-ph/0406278](https://arxiv.org/abs/hep-ph/0406278), doi:10.1103/PhysRevC.71.064901.
- [59] T. Gaitanos, A. B. Larionov, H. Lenske, U. Mosel, Breathing mode in an improved transport approach, *Phys. Rev. C* 81 (2010) 054316. [arXiv:1003.4863](https://arxiv.org/abs/1003.4863), doi:10.1103/PhysRevC.81.054316.
- [60] R. Wang, Z. Zhang, L.-W. Chen, C. M. Ko, Y.-G. Ma, Constraining the in-medium nucleon-nucleon cross section from the width of nuclear giant dipole resonance, *Phys. Lett. B* 807 (2020) 135532. [arXiv:2007.12011](https://arxiv.org/abs/2007.12011), doi:10.1016/j.physletb.2020.135532.
- [61] Y.-D. Song, R. Wang, Z. Zhang, Y.-G. Ma, Nuclear giant quadrupole resonance within a transport approach and its constraint on the nucleon effective mass, *Phys. Rev. C* 104 (4) (2021) 044603. [arXiv:2109.07092](https://arxiv.org/abs/2109.07092), doi: 10.1103/PhysRevC.104.044603.
- [62] Y.-D. Song, R. Wang, Z. Zhang, Y.-G. Ma, In-medium nucleon-nucleon cross sections from characteristics of nuclear giant resonances and nuclear stopping power, *Phys. Rev. C* 108 (6) (2023) 064603. doi:10.1103/PhysRevC.108.064603.
- [63] R. Wang, Y.-G. Ma, L.-W. Chen, C. M. Ko, K.-J. Sun, Z. Zhang, Kinetic approach of light-nuclei production in intermediate-energy heavy-ion collisions, *Phys. Rev. C* 108 (3) (2023) L031601. [arXiv:2305.02988](https://arxiv.org/abs/2305.02988), doi: 10.1103/PhysRevC.108.L031601.
- [64] R. Wang, Z. Zhang, Y.-G. Ma, L.-W. Chen, C. M. Ko, K.-J. Sun, Alpha clustering in warm and dense nuclear matter from heavy-ion collisions (7 2025). [arXiv:2507.16613](https://arxiv.org/abs/2507.16613).
- [65] J. Adamczewski-Musch, et al., Directed, Elliptic, and Higher Order Flow Harmonics of Protons, Deuterons, and Tritons in Au + Au Collisions at $\sqrt{s_{NN}} = 2.4$ GeV, *Phys. Rev. Lett.* 125 (2020) 262301. [arXiv:2005.12217](https://arxiv.org/abs/2005.12217), doi: 10.1103/PhysRevLett.125.262301.
- [66] J. Adamczewski-Musch, et al., Proton, deuteron and triton flow measurements in Au+Au collisions at $\sqrt{s_{NN}} = 2.4$ GeV, *Eur. Phys. J. A* 59 (4) (2023) 80. [arXiv:2208.02740](https://arxiv.org/abs/2208.02740), doi:10.1140/epja/s10050-023-00936-6.
- [67] S. Hama, B. C. Clark, E. D. Cooper, H. S. Sherif, R. L. Mercer, Global Dirac optical potentials for elastic proton scattering from heavy nuclei, *Phys. Rev. C* 41 (1990) 2737–2755. doi:10.1103/PhysRevC.41.2737.
- [68] E. D. Cooper, S. Hama, B. C. Clark, R. L. Mercer, Global Dirac phenomenology for proton nucleus elastic scattering, *Phys. Rev. C* 47 (1993) 297–311. doi:10.1103/PhysRevC.47.297.
- [69] H. Feldmeier, J. Lindner, Field dependent coupling strength for scalar fields, *Z. Phys. A* 341 (1991) 83–88. doi:10.1007/BF01281277.
- [70] N. M. Hugenholtz, L. van Hove, A theorem on the single particle energy in a Fermi gas with interaction, *Physica* 24 (1958) 363–376. doi:10.1016/S0031-8914(58)95281-9.
- [71] L. Satpathy, V. Maheswari, R. Nayak, Finite nuclei to nuclear matter: a leptodermous approach, *Physics Reports* 319 (3) (1999) 85–144. doi:[https://doi.org/10.1016/S0370-1573\(99\)00011-3](https://doi.org/10.1016/S0370-1573(99)00011-3). URL <https://www.sciencedirect.com/science/article/pii/S0370157399000113>
- [72] R. Chen, B.-J. Cai, L.-W. Chen, B.-A. Li, X.-H. Li, C. Xu, Single-nucleon potential decomposition of the nuclear symmetry energy, *Phys. Rev. C* 85 (2012) 024305. [arXiv:1112.2936](https://arxiv.org/abs/1112.2936), doi:10.1103/PhysRevC.85.024305.
- [73] B.-J. Cai, F. J. Fattoyev, B.-A. Li, W. G. Newton, Critical density and impact of $\Delta(1232)$ resonance formation in neutron stars, *Phys. Rev. C* 92 (1) (2015) 015802. [arXiv:1501.01680](https://arxiv.org/abs/1501.01680), doi:10.1103/PhysRevC.92.015802.
- [74] A. Drago, A. Lavagno, G. Pagliara, D. Pigato, Early appearance of Δ isobars in neutron stars, *Phys. Rev. C* 90 (6) (2014) 065809. [arXiv:1407.2843](https://arxiv.org/abs/1407.2843), doi:10.1103/PhysRevC.90.065809.
- [75] V. S. Uma Maheswari, C. Fuchs, A. Faessler, Z. S. Wang, D. S. Kosov, Role of isospin dependent mean field in pion production in heavy ion reactions, *Phys. Rev. C* 57 (1998) 922–926. [arXiv:nucl-th/9708047](https://arxiv.org/abs/nucl-th/9708047), doi: 10.1103/PhysRevC.57.922.

- [76] V. Flaminio, W. G. Moorhead, D. R. O. Morrison, N. Rivoire, *Compilation of Cross-sections. 3. P and \bar{P} Induced Reactions* (4 1984).
- [77] A. Baldini, V. Flaminio, W. G. Moorhead, D. R. O. Morrison, *Total Cross-Sections for Reactions of High Energy Particles (Including Elastic, Topological, Inclusive and Exclusive Reactions) / Totale Wirkungsquerschnitte für Reaktionen hochenergetischer Teilchen (einschließlich elastischer, topologischer, inklusiver, Vol. 12b of Landolt-Boernstein - Group I Elementary Particles, Nuclei and Atoms, Springer, 1988.* doi:10.1007/b35211.
- [78] J. Weil, et al., Particle production and equilibrium properties within a new hadron transport approach for heavy-ion collisions, *Phys. Rev. C* 94 (5) (2016) 054905. arXiv: 1606.06642, doi:10.1103/PhysRevC.94.054905.
- [79] J. Cugnon, J. Vandermeulen, D. L'Hote, Simple parametrization of cross-sections for nuclear transport studies up to the GeV range, *Nucl. Instrum. Meth. B* 111 (1996) 215–220. doi:10.1016/0168-583X(95)01384-9.